



A Kinetic Study of Removing Methylene Blue from Aqueous Solutions by Modified Electrospun Polyethelene Terephthalate

Nanofibres



CrossMark

Hozaan A. Ahmed(1), Parween H. Saleem(2), Suhad A. Yasin(2)*, Ibtisam A. Saeed(2)
 1- Pharmacy Department, Technical Institute Duhok, Duhok Polytechnic University, Iraq(1).
 2- Department of Chemistry, College of Science, University of Duhok, Iraq (2).

Abstract

The present research study investigates the potential use of the novel polyethylene terephthalate (PET) nanofibers extracted from waste bottles. The electrospinning process creates nanofibers which are then impregnated with dibenzo-18-crown-6 (DB18C6) (crown ether) to obtain a modified PET nanofiber. The use of modified PET nanofibers to remove methylene blue (MB) from aqueous solutions at different contact times, temperatures and initial dye concentrations is the prime concern of the present study. The amount of MB adsorbed at equilibrium (q_e) is calculated at different temperatures (303, 313, and 323 K) and different concentrations (5, 10, 15 mg/g). The Kinetic and equilibrium studies of MB removal are carried out. The results indicate that the adsorption kinetics of MB can be described by the pseudo-second-order model. The activation energy value is below 40 kJ/mol and this gives an idea about the physisorption process.

Keywords: Electrospinning; Nanofibers; polyethylene terephthalate (PET); Adsorption; Dibenzo-18-Crown-6 (DB18C6).

1 Introduction

In 1876, methylene blue MB was synthesized as an aniline-based dye in the textile industry. It was mainly used for dyeing paper, silk, leather and cosmetics. MB is basically used as a volumetric analysis indicator. In addition, it is of vital importance as a chemotherapy agent for human and animal medicine[1]. Recently, MB has been proved to serve as a potent reversible monoamine oxidase (MAO) inhibitor with a strong preference for inhibiting MAO-A. Since the inhibition constant is within the nanomolar range, even small doses of MB (less than 1 mg/kg) may inhibit MAO in a clinically significant way. This effect is intensified by the rapid absorption of MB in the nervous tissue, where the concentration of MB in the brain is 10 times greater than in the serum in rat models, which, therefore, can lead to severe side-effects[2].

Various conventional methods such as physical, chemical and biological processes have been used to remove dyes from aquatic media. These processes

include photocatalytic MB dye degradation[3][4], electrochemical oxidation and ozonation processes[5].

Adsorption processes are desirable among the aforementioned methods due to their high performance, low cost, availability and easy design[6]. Attempts have been made to find alternative low-cost adsorbents [7], such as adsorbents used from agricultural solids, including orange peels[8], wheat straw[9], soybean meal hulls[10] or the transformation of agricultural waste into active carbon and its use as adsorbents thereof, such as in the case of jute fibers[11], rice husks[12], activation date holes[13], bamboo dust, coconut shells, peanut shells, straw[14] and corn husks[15].

The applications of single-use disposable on one hand uses nearly 50 per cent of plastics in such industries as packaging, agricultural films and disposable consumer items. On the other hand, the long-term infrastructure industries such as manufacturing pipes, cable coating and other heavy structural materials utilize 20-25% of plastics. The remainder goes directly to intermediate lifespan

*Corresponding author e-mail: Suhad.yasin@uod.ac

Receive Date: 23 December 2020, Revise Date: 12 January 2021, Accept Date: 21 March 2021

DOI: 10.21608/EJCHEM.2021.54843.3146

©2021 National Information and Documentation Center (NIDOC)

durable consumer applications like the manufacture of electronic devices, furniture, vehicles, etc. It is worth mentioning here that Post-consumer plastic waste across the European Union (EU) mounted up to approximately 24.6 million tons in 2007[16].

Plastics have been being recycled since the 1970s. However, the quantities that are recycled vary geographically according to plastic type and application. In fact, Recycling packaging materials has seen rapid expansion over the last decades in a number of countries[17].

In recent years, nanofiber technology has been one of the most important research topics in the field of pollutant removal[18]. This is due to the fact that electrospun nanofiber membranes are excellent adsorbent materials because of their high surface area, porous structure and strong mechanical properties[19][20].

Electrospinning is a very promising, extremely simple, efficient and inexpensive technique used in the manufacturing of nanofibers using a wide variety of polymers [21]. This work introduces the concept of crown ether PET nanofibers for the selective extraction of MB from aqueous solutions. The modification of crown ether PET nanofibers enhances the operating window of electrospun nanofibers and introduces a specific selectivity, making them promising and more effective for adsorption and filtration applications.

In this paper, four kinetic adsorption models are used to describe the experimental data. The study of adsorption dynamics describes the solute uptake rate which evidently controls the residence time of adsorbate uptake at the solid-solution interface. The kinetics of MB dye adsorption on modified PET nanofibers are analyzed using pseudo-first-order, pseudo-second-order Elovich and intra-particle diffusion kinetic models[22]. Each model has its limitations and is derived according to certain conditions[23].

2 Experiment

2.1 Chemicals

Being one of the waste materials, the Polymer (PET) is obtained from a local water packaging company. It is used after being washed, having non-PET materials removed, and then is dried.

All primary chemicals used in this research are of analytical reagent grade. Trifluoroacetic acid (TFA) is obtained from (ROTH), dichloromethane (DCM) from

(UNI-CHEM), Dibenzo-18-crown-6 (DB18C6) from (SIGMA-ALDRICH), Methylene blue (MB) from (SIGMA) and Acetone from (TEDIA).

2.2 Preparation of Solution

A PET polymer solution was prepared by mixing in a 3:1 ratio of dichloromethane and trifluoroacetic acid; three specific PET concentrations are used in this study[24]. Five percent-PET was used to produce the desired product. PET was grinded with (GRAND Household) and then sifted with (TESTSIEVE 250 mm). The solution was stirred to complete the dissolution of PET using a magnetic stirrer at room temperature for four hours to supplement the PET solubility[4].

In 100 ml of deionized water, a stock solution of MB(1000 mg/L) is obtained by dissolving 0.1 g of MB, and the solution is used for further experimental solution preparation. With 1 M HCL or 0.6 M NaOH, the pH values are adjusted. Throughout this preparation, deionized water is used in adsorption experiments.

2.3 Preparation and Modification of PET Nanofibers with DB18C6

The polymer solution was converted into nanofibers by the electrospinning device Micro-nanotools, as shown in a previous study's optimization[24].

Then a 0.011 g PET nanofiber mat was impregnated with 0.02g of DB18C6 dissolved in 6 mL of acetone with continuous stirring at ambient temperature for two hours. After two hours, the mat was washed with deionized water several times to remove any free ions and then dried at room temperature for one hour.

2.4 Batch Adsorption Studies of MB

In a batch process, MB adsorption was achieved by varying contact time, adsorbate concentration, and temperature.

A weighed sample of dried modified PET nanofibers was mixed with a 10 ml MB solution and the pH was adjusted. The mixture was shaken in the water bath of a thermostat for 100 minutes at 150 rpm. The mixture was allowed to settle and then centrifuged. The MB concentration in the supernatant was determined with a spectrophotometer type (JANEWAY 7315 Spectrophotometer) from the contrast calibration curve.

Table 1. Kinetic and Equilibrium Equations

| Kinetic models | Kinetic equation | | Reference |
|---|---|--|---------------------------------------|
| q_e = adsorbed MB (mg/g) at equilibrium | $q_e = \frac{C_o - C_e}{M}$ | C_i, C_e = Initial and equilibrium concentration (mg/L) of MB in the solution. V = Volume of experimental solution (L), M = Weight of the modified PET used (g). | [18],[25],[26],[27] |
| Adsorption Efficiency (R%) | $R\% = \frac{C_o - C_e}{C_o} \times 100$ | | [27],[28] |
| Pseudo first- order | $\log(q_e - q_t)$ $= \log q_e - \left(\frac{k_1}{2.303}\right)t$ | q_e = Amount of MB adsorbed (mg/g) at any time, t (min) q_t = Amount of MB adsorbed (mg/g) at equilibrium. k_1 = The first order equilibrium rate constant. t = Time | [29], [30],[28], [31],[32] |
| Pseudo-second- order | $\frac{t}{q_t} = \frac{1}{k_2 q_e^2} + \frac{1}{q_e} (t)$ | k_2 = The second order equilibrium rate constant. h = Initial adsorption rate in the pseudo-second order kinetic. | [27], [28],[29], [30],[31], [32] |
| Elovich kinetic model | $q_t = \frac{1}{\beta} \ln(\alpha\beta) + \frac{1}{\beta} \ln(t)$ | α =Initial adsorption rate(mg/g ^{1/2}) β =Desorption constant (g.mg ⁻¹) | [29],[30], [27] |
| Intra.Particle diffusion | $q_t = K_{dif} t^{\frac{1}{2}} + B_L$ | K_{dif} = (mg/g.min) The intraparticle diffusion rate constant. B_L = The thickness of the boundary layer, | [18], [33],[30], [28],[31], [34],[32] |
| Activation energy (E_a) | $k = k_o \exp(-E_a/RT)$ | k = Sorption (g/mg min) rate k_o =Arrhenius constant (temp independent factor) (g/mg min), E_a = Activation energy (kJ/mol), R = Gas constant (8.314 J/mol K) T = Solution temperature Kelvin (K). | [18], [28],[32] |

2.4.1 Effect of Contact Time and Temperature on Adsorption

The effect of temperature on the adsorption of MB onto modified PET nanofibers was performed by mixing 10 ml of MB solution 10 mg/L at pH 6 and 0.02g of modified PET nanofibers at temperatures (303, 313 and 323 K) and shacked with 150 rpm for (5, 10, 20, 30, 40, 50, 60, 70, 80, 90, 100, 120, 140 minutes).

2.4.2 Effect of Contact Time and MB Concentration on Adsorption

The effect of the initial concentration on the adsorption of MB to modified PET nanofibers was achieved by mixing 10 ml of varied initial MB concentrations (5, 10, 15 mg/L) at pH 6 and 0.02 g of modified PET nanofibers at 313 K and shaking at 150 rpm for 5, 10, 20, 30, 40, 50, 60, 70, 80, 90, 100, 120 and 140 minutes.

2.5 Adsorption Kinetic Investigation

The equations in (Table 1) are used to calculate q_e (mg/g) that related to the amount of MB adsorbed onto the modified PET nanofibers and the MB removal percent (R%).

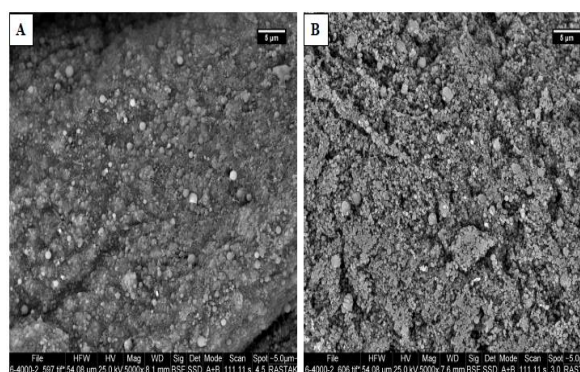


Fig 1. SEM Micrographs of PET nanofiber A; before B; after modification

The adsorption capability nature is clearly demonstrated by the adsorption kinetics over time. It is a prerequisite to identify the type of adsorption mechanism in a particular system. The four kinetics

models used to describe the behavior of adsorption kinetics of MB on modified PET nanofibers include the pseudo-first-order, pseudo-second-order, Elovich models and intraparticle diffusion. Table (1) shows the final kinetic equations used in this study.

3 Results and Discussion

SEM characterized PET nanofiber's morphologies before and after modification as shown in figure 1. One of the most critical parameters for the adsorption capability determination of the nanofibers is the Brunauer–Emmett–Teller surface area (BET). The highly specialized surface area, fast diffusion rates through hydrophilic mesopores, and the electrostatic attractions between the surface nanofibers and dyes all lead to a rapid and efficient purification. Figure 2 shows the nitrogen adsorption-desorption isotherms showing the hysteresis loops, indicating the presence of mesopores. Based on BET analysis, the surface area of PET nanofibers is $22.282\text{m}^2/\text{g}$ and the total pore volume is $(0.01846\text{cm}^3/\text{g})$ as shown in the results below.

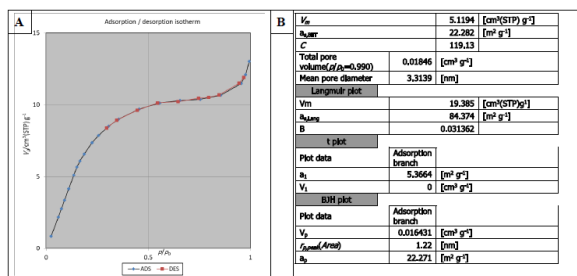


Fig 2. Nitrogen Adsorption–Desorption Isotherms for PET Nanofibers

The Fourier Transform Infrared Spectroscopy (FTIR) analysis has been used for the examination of functional groups on the surface of adsorbent[35].

The bands of the modified PET nanofiber adsorbent as shown in figure (3A) are located at 1241cm^{-1} that indicates the stretching frequencies $\nu_{\text{as}}(\text{Ph-O-C})$ in crown ether, (waging of aromatic hydrocarbon) at 720cm^{-1} [36], at 1634cm^{-1} (C=C stretch), 1596 , 1496 , and 1456 (C=C aromatic ring stretch) with respect to aromatic ring absorbance[37]. The disappearance of these peaks in presented in figure (3B) may be attributed to the adsorption of methylene on modified PET nanofibers by weak electrostatic, face-to-face, π - π interactions between the aromatic moieties. The stabilizing energy of π - π interactions also includes induced dipole and dispersion contributions[38][39].

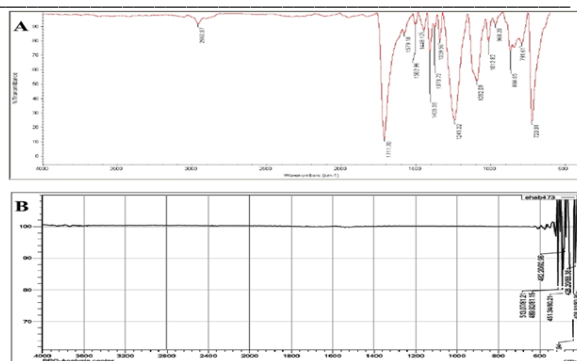


Fig 3. FTIR Spectra of Modified PET Nanofiber A; Before B; After Adsorption of MB

3.1 The Effect of Contact Time and Temperature on Adsorption

Figure (4) illustrates a plot of the adsorbed amount of MB q_e (mg/g) vs. contact time at varying temperatures (303 , 313 and 323K). It is observed that the amount of MB uptake, q_t (mg/g) which has increased rapidly during the first 10 minutes at all degrees of temperature represents the film diffusion. After 10 minutes, the amount of MB adsorbed increased gradually at a slower rate, at 303 and 313K , represents the pore diffusion, and finally attained equilibrium at 100 min. At 323K , however, there was a sharp increase in the amount of MB uptake, q_t (mg/g), until it reached 100 minutes. The equilibrium was reached after 100 minutes. These three steps are in accordance with those reported in the research literature and they clearly illustrate the adsorption process mechanism[40]. Further, the amount of MB adsorbed increased with an increase in temperature. These observations show that the temperature does not affect equilibrium time.

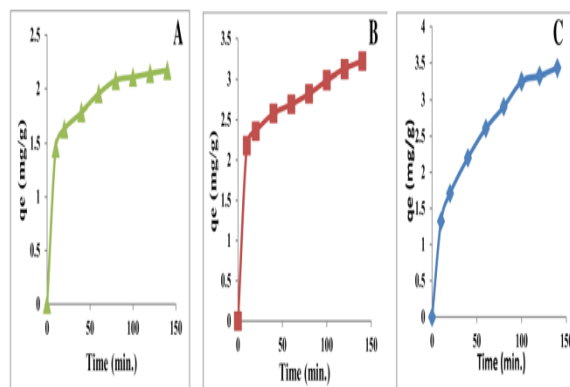


Fig 4. Effect of contact time and temperature on the adsorption of MB on modified PET nanofiber. A; 303K , B; 313K , C; 323K

3.2 The Effect of Contact Time and MB Concentration on Adsorption

The initial MB concentration can be seen as a significant impetus to resolve any MB molecules resistance to mass transfer between the aqueous and solid phases. Therefore, a higher initial MB concentration increases the adsorption capacity q_e . When the initial 5.0 mg/L dye concentration goes up to 15 mg/L, the 2.590 mg/g equilibrium sorption capacity mounts up to 4.506 mg/g.

MB adsorption on modified PET nanofibers as a function of contact time at different initial concentrations is shown in figure. 5. The results show that the adsorption rate of all concentrations was rapid in the first ten minutes and gradually steadily with increasing contact time until equilibrium was reached. The adsorption rate was also observed during the first ten minutes. It increased significantly with increasing MB concentration, the reason being that higher concentration leads to enhanced momentum along with pores, which leads to increased absorption capacity[41].

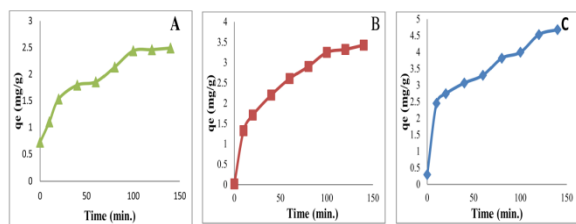


Fig 5. Effect of contact time and MB concentration on the adsorption of MB on modified PET nanofiber. A; 5mg/L, B; 10 mg/L, C; 15 mg/L

3.3 Adsorption Kinetic Study

Four kinetic models are used to estimate the sorption mechanism and possible rate-controlling steps, which are essential in selecting optimum operating conditions for the full batch process.

At different MB concentrations and temperatures, the adsorption capacity of MB onto modified PET nanofibers is monitored as a function of time until constant MB amount of adsorbed is reached. The process implies that the equilibrium is reached. Equilibrium time is 100 minutes in all degrees of concentration and temperature under study.

The equilibrium adsorption capacity of MB onto modified PET nanofibers (q_e) increases proportionally with the increase in the initial MB concentrations and temperatures. The equilibrium adsorption capacity

values obtained under all experimental conditions are presented in Tables 2–3.

3.3.1 The Effect of Temperature on Adsorption Kinetics

Figure 6 demonstrates the effect of temperature on pseudo-first-order adsorption kinetics of MB on modified PET nanofibers.

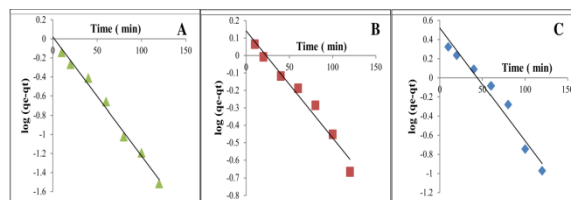


Fig 6. Pseudo-first order adsorption kinetics of the adsorption of MB on modified PET nanofiber at different temperature. A; 303 K, B;313K, C;323K

In spite of the high values of the correlation coefficients R^2 scored with the experimental data (>0.958), the calculated values of the equilibrium sorption capacity q_t , do not actually agree with the experimental data as demonstrated by (Table 2). This in turn indicates the applicability shortcoming of the pseudo-first order model in the prediction of the MB adsorption kinetics on modified PET nanofiber.

Figure (7) illustrates the effect of temperature on pseudo-second-order sorption kinetics of MB onto modified PET nanofibers. As shown in Table (2), the values of K_2 decrease with the increasing temperature.

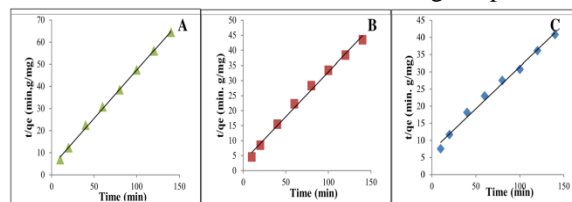


Fig 7. Pseudo-second order adsorption kinetics of the adsorption of MB on modified PET nanofiber at different temperature. A; 303 K, B;313K, C;323K

The calculated R^2 -values are found to be higher than (0.995) for all of the temperature degrees. The computed values of the equilibrium sorption capacity q_e , go in agreement with the experimental data, q_e , at 303 and 313 K. accordingly, this indicates that the removal of MB onto modified PET nanofibers follows the pseudo-second-order equation at these temperatures. However, at 323 K, deviation will occur. The pseudo-second-order can be concluded that the process is due to chemical adsorption (chemisorption) where MB dye attaches to the modified PET nanofiber, through the formation of a chemical bond and searches for the active sites that can maximize

their coordination number with the surface [40]. The Elovich equation is a rate equation based on the adsorption capacity commonly expressed in Table (1). Figure (8) depicts a plot of q_t versus $\ln(t)$. The Elovich constants α and β were obtained from the intercept and slope, respectively, and reported in Table 3.

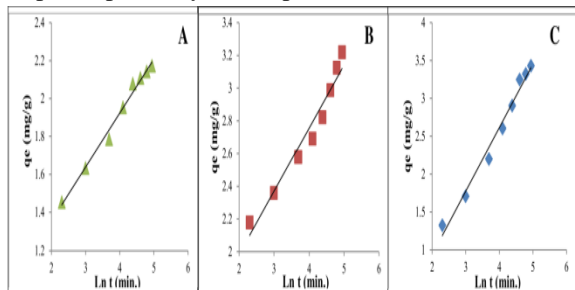


Fig 8. Elovich kinetic for the adsorption of MB on modified PET nanofiber at different tempreure. A; 303 K, B;313K, C;323K

If MB adsorption by modified PET nanofibers fits the Elovich model, a plot of q_t versus $\ln(t)$ should yield a linear relationship with the high values of the correlation coefficients, R^2 , (>0.958).

The initial adsorption rate α increased from 5.375 to 8.953 $(\text{mg/g min})^{-1}$ with an increase in the temperature from 303 to 313 K, and it decreased at 323 K to 2.031 $(\text{mg/g min})^{-1}$. A similar pattern is mentioned above for the initial adsorption rate, h , obtained from the pseudo-second-order model. The desorption constant, β , decreased from 3.874 to 1.191 g.mg^{-1} with an increase in temperature (Table 3).

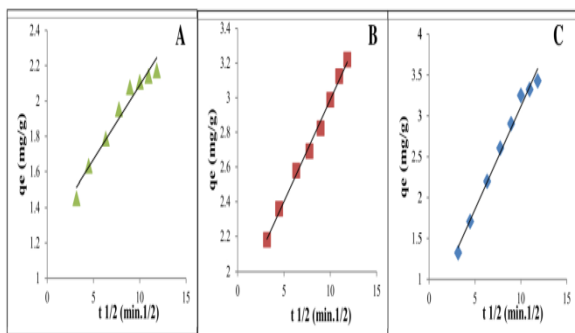


Fig 9. Intraparticle diffusion for the adsorption of MB on modified PET nanofiber at different tempreure. A; 303 K, B;313K, C;323K

Figure (9) shows the temperature effect on the MB intraparticle diffusion kinetics. The values of K_{dif} proportionally increase as temperature goes high. The value of R^2 from the plot given in figure 8 is 0.9952 at 313 K.

3.3.2 The Effect of Initial MB Concentration on Adsorption Kinetics

Figure (10) provides a demonstration of the pseudo first-order sorption kinetics for the adsorption of MB

onto modified PET nanofibers at a divergent range of the initial dye concentrations and also of the 313 K. The rate of the constant values obtained from the pseudo-first-order model declines with the gradual increase in the initial concentrations of the dye.

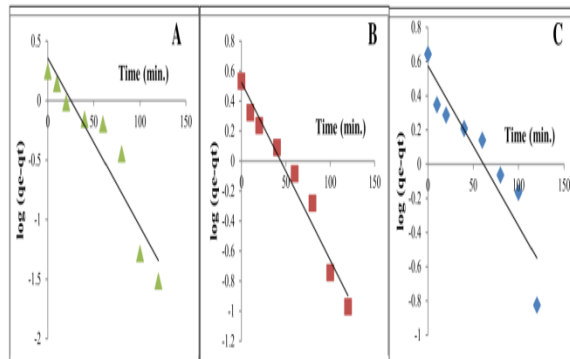


Fig 10. Pseudo-first order sorption kinetics of the adsorption A; 5mg/L , B; 10 mg/L, C; 15 mg/L of MB on modified PET nanofiber.

The calculated q_e , k_1 and the corresponding linear regression correlation coefficient R^2 values are shown in Table 2. It was observed that the correlation coefficient R^2 is relatively low for most adsorption data, and the calculated q_e at 15 mg/L does not agree with experimental values. This shows no applicability of the pseudo-first-order model in predicting the kinetics of the MB adsorption onto modified PET nanofibers.

Figure (11) shows the pseudo-second-order adsorption kinetics of MB onto modified PET nanofibers for different initial dye concentrations at 313 K and 150 rpm. For all initial dye concentrations, a straight line was obtained with correlation coefficient R^2 values higher than R^2 values for pseudo-first-order kinetics.

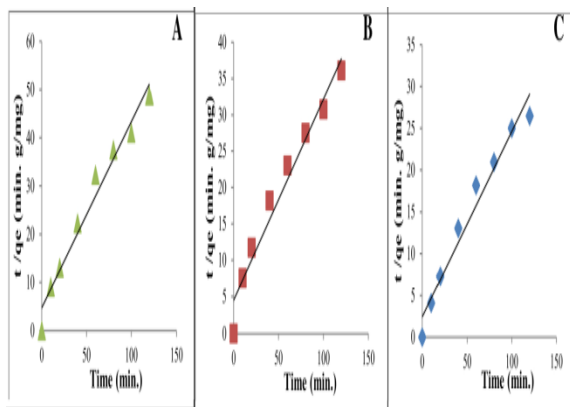


Fig 11. Pseudo-second order sorption kinetics of the adsorption A; 5mg/L , B; 10 mg/L, C; 15 mg/L of MB on modified PET nanofiber.

As shown in Table 2, the values of the initial sorption rate, h , and the values of the rate constant obtained from pseudo-second-order kinetics, k_2 ,

Table 2:- Pseudo-first-order and Pseudo-second-order kinetic parameters of adsorption of MB on modified PET nanofiber at different temperatures and different initial MB concentrations.

| | $q_{e(\text{exp.})}$ | Pseudo-first-order | | | Pseudo-second-order | | | |
|---------|----------------------|--------------------|--------|-----------------------|---------------------|-------|--------|-----------------------|
| | | R^2 | K_1 | $q_{e(\text{calc.})}$ | R^2 | h | K_2 | $q_{e(\text{calc.})}$ |
| 303 K | 2.172 | 0.9626 | 0.0287 | 1.047 | 0.9987 | 0.270 | 0.1180 | 2.289 |
| 313 K | 3.219 | 0.9691 | 0.0140 | 1.384 | 0.9937 | 0.326 | 0.0974 | 3.351 |
| 323 K | 3.429 | 0.9892 | 0.0271 | 3.313 | 0.9904 | 0.143 | 0.0352 | 4.071 |
| 5 mg/L | 2.491 | 0.8981 | 0.0327 | 2.276 | 0.9703 | 0.211 | 0.0815 | 2.590 |
| 10 mg/L | 3.429 | 0.9717 | 0.0274 | 3.346 | 0.9635 | 0.223 | 0.0618 | 3.611 |
| 15 mg/L | 4.682 | 0.8699 | 0.0216 | 3.755 | 0.9667 | 0.408 | 0.0906 | 4.506 |

This rise in the initial sorption rate suggests that in high concentrations, the solute and sorbet molecules can be encountered more with each other. In addition, the value of $q_{e(\text{calc.})}$ is in good agreement with $q_{e(\text{exp.})}$, which indicates that the removal of MB onto modified PET nanofibers follows the pseudo-second-order equation.

Figure 12 depicts the plot of q_t versus $\ln(t)$ and the Elovich constants α and β were obtained from the intercept and slope, respectively, and are reported in Table 5. The correlation coefficient R^2 is comparable to the correlation coefficients obtained for the

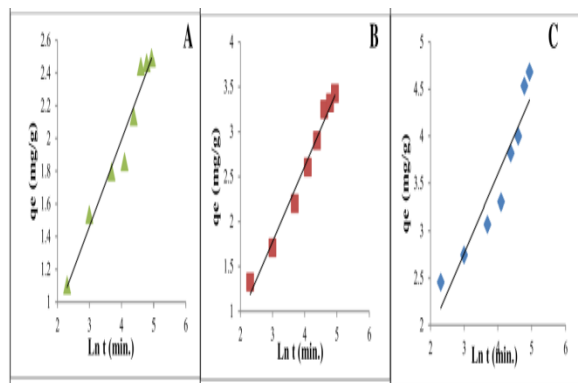


Fig 12. Elovich kinetic for the adsorption A; 5mg/L, B; 10 mg/L, C; 15 mg/L of MB on modified PET nanofiber.

pseudo-second-order model for 5 and 10 mg/L. This reflects the applicability of this model to the experimental data obtained for the adsorption of MB on modified PET nanofibres.

The obtained values that indicate the rates of the intra-particle diffusion can be estimated from the plots slopes of q_t against $t^{1/2}$ (figure13). The intraparticle diffusion rate constant K_{dif} increased with an increase in initial concentration, as shown in Table 3. The obtained R^2 -values are 0.9613, 0.9879 and 0.9724 for

increased with the increase in the initial concentrations of the dye.

the initial concentrations of the dye of 5.0, 10 and 15 mg/L, respectively.

The linearity of the plots (figure 9 and figure13) showed that intra-particle diffusion played a major role in the uptake of the MB by modified PET nanofibres.

This also confirms that the adsorption of the MB on modified PET nanofibres was a multi-step process into the interior.

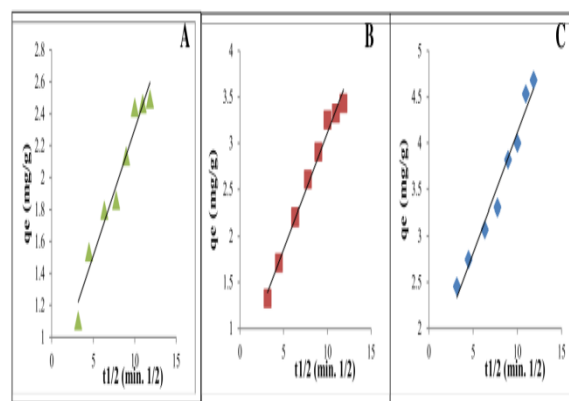


Fig 13. Intraparticle diffusion for the adsorption A; 5mg/L, B; 10 mg/L, C; 15 mg/L of MB on modified PET nanofiber.

If the steps are separate from each other, the plot usually shows two or more intersecting lines depending on the exact mechanism, the first one representing surface adsorption and the second one representing intraparticle diffusion.

The absence of such features in the plots indicates that the steps were indistinguishable from one another and that the intra-particle diffusion was a prominent process right from the beginning of the MB/modified PET nanofiber interaction.

However, this does not give a sufficient indication about which of the two steps was the rate-limiting step.

Table 3: - Elovich kinetic, Intraparticle diffusion kinetic parameters of adsorption of MB on modified PET nanofiber at different temperatures and different initial MB concentrations.

| | Elovich Kinetic | | | Intraparticle Diffusion | | |
|---------|-----------------|----------|----------|-------------------------|-------------------|----------------|
| | R ² | α | β | R ² | K _{diff} | B _L |
| 303 K | 0.9893 | 5.357 | 3.8744 | 0.9618 | 0.0842 | 1.2483 |
| 313 K | 0.9568 | 8.953 | 2.5933 | 0.9952 | 0.1178 | 1.8114 |
| 323 K | 0.9830 | 2.031 | 1.1916 | 0.9879 | 0.2520 | 0.5955 |
| 5 mg/L | 0.9638 | 0.67 | 1.890359 | 0.9613 | 0.1582 | 0.7226 |
| 10 mg/L | 0.983 | 2.031 | 1.191611 | 0.9879 | 0.252 | 0.5955 |
| 15 mg/L | 0.8982 | 1.139 | 1.198753 | 0.9724 | 0.26 | 1.5142 |

It is also essential for the q_t versus $t^{1/2}$ plots to navigate the origin if the diffusion of the intra-particle is the only rate-limiting step.

Since this was also not the case in both figure. 9 and figure. 13, it may be concluded that surface adsorption and intra-particle diffusion were concurrently operating during the MB/modified PET nanofiber interaction.

In addition, the intercept B_L reveals a fact that in boundary layer thickness, the more the value of the intercept gets high, the greater effect the boundary layer has [31]. In other words, as the intercept B_L increases in results, the abundance of the solute adsorbed on the boundary layer grows higher. Table 3 includes the values of B_L which are obtained from the intercept of the linear plots of q_t vs $t^{1/2}$ under all the conditions under study.

As a result, it is clear that the values of the correlation coefficients obtained for the linear plots from the pseudo-second-order equation are greater than those obtained for the first order and intra-particle diffusion equations under all conditions studied, as shown in Tables 2–3 indicates that the intra-particle diffusion rate is one of the rate-determining steps.

Moreover, the equilibrium sorption capacity values (q_e) considerably agree with the experimental data, (q_e). this agreement strongly results in an activated sorption between the functional groups and the dye on the modified PET nanofibers, involving valency forces through sharing or exchanging electrons between MB and the modified PET nanofibers.

Also, the results show that the adsorption rate of all concentrations and temperatures is rapid in the first ten minutes and this is one of the advantages of the modified PET nanofibers compared with the previous studies, as shown in table 4.

3.4 Activation Energy

The activation energy of the adsorption for MB onto a modified PET nanofiber system can be estimated by the Arrhenius equation providing the relationship between rate constant and temperature, as shown in Table 1.

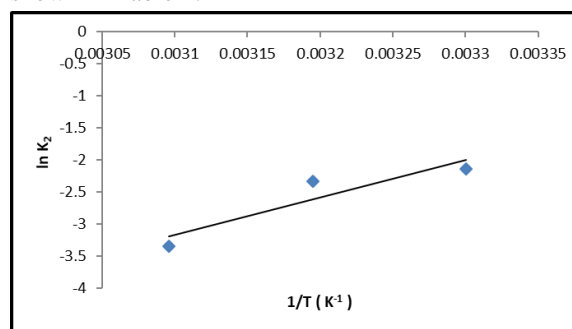


Fig 14. A plot of $\ln K_2$ versus $1/T$ for the adsorption of MB on modified PET nanofiber.

In this research study, the activation energy of the adsorption process has been calculated using the values of the rate constant from the pseudo-second-order kinetic equation and the appropriate solution temperatures[47]. An Arrhenius plot drawn of $\ln K_2$ versus $1/T$ is shown in figure14. The value of E_a from the slope of the plot is -48.762 kJ/mol. In the comparable analysis, it has been observed that the activation energy is -8.0 kJ/mol for the biosorption

of cadmium (III) ion onto dried *C. Vulgaris*, -15.65 kJ/mol for adsorption of Cr(III) ions on vineyard pruning waste (VPW) [48]and -13.9 kJ/mol for the biosorption of nickel(II) ion onto deactivated protonated yeast[49].

The magnitude of the activation energy provides an understanding of the adsorption process which is mainly physical or chemical. This implies that the adsorption has a potential barrier comparable to physisorption as the activation energy values are below 40 kJ/mol.

Table 4: Summary of adsorption kinetics compared with other related studies from the literature

| Adsorbent | Absorbent | Equilibrium time | Ref. |
|-------------------|-----------|------------------|---------------|
| PET bottle wastes | MB | 80 min. | [42] |
| PET bottle wastes | MB | 3 days | [43] |
| PET bottle wastes | MB | 30 min. | [44] |
| PET bottle wastes | MB | 45-60 min. | [45] |
| PET bottle wastes | MB | 30 min | [46] |
| PET bottle wastes | MB | 10 min | Current Study |

4 Conclusions

The present research study shows that the modified PET nanofibers constructed by waste bottles can be used as an adsorbent for the removal of MB from the aqueous solutions after chemical modification. It was found that the amount of dye adsorbed varies with the adsorbent contact time, temperature and initial dye concentration. The results show that the adsorption rate for all concentrations is rapid during the first ten minutes and gradually progress with the increase in the contact time until reaching the equilibrium. This is one of the advantages of the modified PET nanofibers compared with previous studies. The adsorption rate is found to correspond with a good correlation with pseudo-second-order kinetics. The magnitude of the activation energy gives an idea that the adsorption has a potential barrier comparable to physisorption since the activation energy value is below 40 kJ/mol.

Acknowledgments

The authors are grateful for the financial support by USAID Partnerships for Enhanced Engagement in Research (PEER) Program – an international grants program that funds scientists and engineers in developing countries who partner with U.S. government-funded researchers to address global development challenges. It was administered by the U.S. National Academies of Sciences, Engineering and Medicine (NASEM), PEER/Iraq project/cycle 6.

5 References:

- [1] Berneth H. Azine dyes, Ullmann's Encyclopedia of Industrial Chemistry. Wiley Online Library (2000).
- [2] Top W.M.; Gillman P.K.; De Langen C.J.; Kooy A. ;Fatal methylene blue associated serotonin toxicity. *Neth J Med*, 72(3): 179–181 (2014).
- [3] Aragaw B.A.; Dagnaw A. ;Copper/reduced graphene oxide nanocomposite for high performance photocatalytic methylene blue dye degradation. *Ethiopian Journal of Science and Technology*, 12(2): 125–137 (2019).
- [4] Yasin S.A.; Abbas J.A.; Ali M.M.; Saeed I.A.; Ahmed I.H. ;Methylene blue photocatalytic degradation by TiO₂ nanoparticles supported on PET nanofibres. *Materials Today: Proceedings*, 20: 482–487 (2020).
- [5] Elahmadi M.F.; Bensalah N.; Gadri A. ;Treatment of aqueous wastes contaminated with Congo Red dye by electrochemical oxidation and ozonation processes. *Journal of Hazardous Materials*, 168(2–3): 1163–1169 (2009).
- [6] Tehrani-Bagha A.R.; Nikkar H.; Mahmoodi N.M.; Markazi M.; Menger F.M. ;The sorption of cationic dyes onto kaolin: Kinetic, isotherm and thermodynamic studies, (2011).
- [7] Mahmoodi N.M.; Mokhtari-Shourijeh Z. ;Preparation of PVA-chitosan blend nanofiber and its dye removal ability from colored wastewater. *Fibers and Polymers*, 16(9): 1861–1869 (2015).
- [8] Sivaraj R.; Namasivayam C.; Kadirvelu K. ;Orange peel as an adsorbent in the removal of acid violet 17 (acid dye) from aqueous solutions. *Waste management*, 21(1): 105–110 (2001).
- [9] Arami M.; Limaee N.Y.; Mahmoodi N.M.; Tabrizi N.S. ;Equilibrium and kinetics studies for the adsorption of direct and acid dyes from aqueous solution by soy meal hull. *Journal of Hazardous Materials*, 135(1–3): 171–179 (2006).
- [10] Senthilkumaar S.; Varadarajan P.R.; Porkodi K.; Subbhuraam C. V. ;Adsorption of methylene blue onto jute fiber carbon: kinetics and equilibrium studies. *Journal of colloid and interface science*, 284(1): 78–82 (2005).

- [11] Bulut Y.;Ayd H.;Aydin H. ;A kinetics and thermodynamics study of methylene blue adsorption on wheat shells. *Desalination*, 194(1–3): 259–267 (2006).
- [12] Malik P.K. ;Use of activated carbons prepared from sawdust and rice-husk for adsorption of acid dyes: a case study of Acid Yellow 36. *Dyes and pigments*, 56(3): 239–249 (2003).
- [13] Banat F.;Al-Asheh S.;Al-Makhadmeh L. ;Evaluation of the use of raw and activated date pits as potential adsorbents for dye containing waters. *Process Biochemistry*, 39(2): 193–202 (2003).
- [14] Kannan N.;Sundaram M.M. ;Kinetics and mechanism of removal of methylene blue by adsorption on various carbons—a comparative study. *Dyes and pigments*, 51(1): 25–40 (2001).
- [15] Khodaie M.;Ghasemi N.;Moradi B.;Rahimi M. ;Removal of methylene blue from wastewater by adsorption onto ZnCl₂ activated corn husk carbon equilibrium studies. *Journal of Chemistry*, 2013 (2013).
- [16] Xie F.;Wang Y.;Zhuo L.;Jia F.;Ning D.;Lu Z. ;Electrospun Wrinkled Porous Polyimide Nano fiber-Based Filter via Thermally Induced Phase Separation for Efficient High-Temperature PMs Capture, (2020).
- [17] Hopewell J.;Dvorak R.;Kosior E. ;Plastics recycling: Challenges and opportunities. *Philosophical Transactions of the Royal Society B: Biological Sciences*, 364(1526): 2115–2126 (2009).
- [18] Naser J.A.;Himdan T.A.;Ibraheim A.J. ;Adsorption kinetic of malachite green dye from aqueous solutions by electrospun nanofiber Mat. *Oriental Journal of Chemistry*, 33(6): 3121–3129 (2017).
- [19] Yalcinkaya F.;Yalcinkaya B.;Hruza J. ;Electrospun Polyamide-6 Nanofiber Hybrid Membranes for Wastewater Treatment. *Fibers and Polymers*, 20(1): 93–99 (2019).
- [20] Yasin S.A.;Abbas J.A.;Saeed I.A.;Ahmed I.H.;Yasin S.A.;Saeed I.A.;*et al.* ;The application of green synthesis of metal oxide nanoparticles embedded in polyethylene terephthalate nanofibers in the study of the photocatalytic degradation of methylene blue, (2019).
- [21] Hou C.;Yang H.;Xu Z.-L.;Wei Y. ;Preparation of PAN/PAMAM blend nanofiber mats as efficient adsorbent for dye removal. *Fibers and Polymers*, 16(9): 1917–1924 (2015).
- [22] Jayajothi C.;Senthamilselvi M.M.;Arivoli S.;Muruganatham N. ;Kinetic, Thermodynamic and Isotherm Studies on the Removal of Methylene Blue Dye using Acid Activated *Glossocardia linearifolia* Stem.
- [23] Al-Ghouti M.A.;Khraisheh M.A.M.;Ahmad M.N.M.;Allen S. ;Adsorption behaviour of methylene blue onto Jordanian diatomite: a kinetic study. *Journal of hazardous materials*, 165(1–3): 589–598 (2009).
- [24] Abbas J.A.;Said I.A.;Mohamed M.A.;Yasin S.A.;Ali Z.A.;Ahmed I.H. ;Electrospinning of polyethylene terephthalate (PET) nanofibers: optimization study using taguchi design of experiment. *IOP Conf Ser Mater Sci Eng*, 454: 12130 (2018).
- [25] Chen D.;Wei L.;Meng L.;Wang D.;Chen Y.;Tian Y.;*et al.* ;High-performance self-powered UV detector based on SnO₂-TiO₂ nanomaterial arrays. *Int J Polym Sci*, 13(1): 92 (2018).
- [26] Yasin S.A.;Qasim A.K. ;Kinetic Study of Adsorption of Hexavalent Chromium in Aqueous Solution using Bay Leaf (*Laurus Nobilis*) as New Bio-Adsorbent. *Science Journal of University of Zakho*, 6(3): 104–107 (2018).
- [27] Liu L.;Fan S.;Li Y. ;Removal behavior of methylene blue from aqueous solution by tea waste: kinetics, isotherms and mechanism. *International journal of environmental research and public health*, 15(7): 1321 (2018).
- [28] Adeyi A.A.;Jamil S.N.A.M.;Abdullah L.C.;Choong T.S.Y.;Lau K.L.;Abdullah M. ;Adsorptive Removal of Methylene Blue from Aquatic Environments Using Thiourea-Modified Poly(Acrylonitrile-co-Acrylic Acid). *Materials*, 12(11): 1734 (2019).
- [29] Chen X.;Song X.;Sun Y. ;Attapulgit nanofiber-cellulose nanocomposite with core-shell structure for dye adsorption. *International Journal of Polymer Science*, 2016: 1–9 (2016).
- [30] Najim T.S.;Yasin S.A.A.R. ;Adsorption of Cr (VI) from Aqueous Solution Using Low Cost Adsorbent: Equilibrium Study. *Science Journal of University of Zakho*, 1(2): 758–767 (2018).
- [31] Zulfikar M.A.;Bahri A.;Nasir M. ;Adsorption of Humic Acid from Aqueous Solution onto PMMA Nanofiber : Kinetics Study. *International*

- Proceedings of Chemical, Biological and Environment Engineering*, 94(19) (2016).
- [32] Acemioğlu B. ;Batch kinetic study of sorption of methylene blue by perlite. *Chemical Engineering Journal*, 106: 73–81 (2005).
- [33] Chen X.;Song X.;Sun Y. ;with Core-Shell Structure for Dye Adsorption. *International Journal of Polymer Science*, 2016 (2016).
- [34] Khaled A.;Nemr A. El;El-sikaily A.;Abdelwahab O. ;Removal of Direct N Blue-106 from artificial textile dye effluent using activated carbon from orange peel: Adsorption isotherm and kinetic studies. *Journal of Hazardous Materials*, 165(1–3): 100–110 (2009).
- [35] Habeeb O.A.;Ramesh K.;Ali G.A.M.;Yunus R.M. ;Isothermal modelling based experimental study of dissolved hydrogen sulfide adsorption from waste water using eggshell based activated carbon. *Malaysian J Anal Sci 2017b*, 21: 334–345 (2017).
- [36] El Nemr A.;Khaled A.;Abdelwahab O.;El-Sikaily A. ;Treatment of wastewater containing toxic chromium using new activated carbon developed from date palm seed. *Journal of Hazardous Materials*, 152(1): 263–275 (2008).
- [37] Dos Santos Pereira A.P.;Da Silva M.H.P.;Lima É.P.;Dos Santos Paula A.;Tommasini F.J. ;Processing and characterization of PET composites reinforced with geopolymer concrete waste. *Materials Research*, 20: 411–420 (2017).
- [38] Ibupoto A.S.;Qureshi U.A.;Ahmed F.;Khatri Z.;Khatri M.;Maqsood M.;*et al.* ;Reusable carbon nanofibers for efficient removal of methylene blue from aqueous solution. *Chemical Engineering Research and Design*, 136: 744–752 (2018).
- [39] Kiviniemi S. ;Complexation of N-Heteroaromatic Cations With Crown Ethers and Tetrapenylborate, (2001).
- [40] Maazinejad B.;Mohammadnia O.;Ali G.A.M.;Makhlouf A.S.H.;Nadagouda M.N.;Sillanpää M.;*et al.* ;Taguchi L9 (34) orthogonal array study based on methylene blue removal by single-walled carbon nanotubes-amine: Adsorption optimization using the experimental design method, kinetics, equilibrium and thermodynamics. *Journal of Molecular Liquids*, 298: 112001 (2020).
- [41] Choo H.S.;Lau L.C.;Mohamed A.R.;Lee K.T. ;Hydrogen sulfide adsorption by alkaline impregnated coconut shell activated carbon. *Journal of Engineering Science and Technology*, 8(6): 741–753 (2013).
- [42] Djahed B.;Shahsavani E.;Khalili Naji F.;Mahvi A.H. ;A novel and inexpensive method for producing activated carbon from waste polyethylene terephthalate bottles and using it to remove methylene blue dye from aqueous solution. *Desalination and Water Treatment*, 57(21): 9871–9880 (2016).
- [43] Lian F.;Xing B.;Zhu L. ;Comparative study on composition, structure, and adsorption behavior of activated carbons derived from different synthetic waste polymers. *Journal of colloid and interface science*, 360(2): 725–730 (2011).
- [44] El Essawy N.A.;Ali S.M.;Farg H.A.;Konsowa A.H.;Elnouby M.;Hamad H.A. ;Green synthesis of graphene from recycled PET bottle wastes for use in the adsorption of dyes in aqueous solution. *Ecotoxicology and environmental safety*, 145: 57–68 (2017).
- [45] de Castro C.S.;Viau L.N.;Andrade J.T.;Mendonça T.A.P.;Gonçalves M. ;Mesoporous activated carbon from polyethyleneterephthalate (PET) waste: pollutant adsorption in aqueous solution. *New Journal of Chemistry*, 42(17): 14612–14619 (2018).
- [46] Rahmawati I.;Priyanto A.;Darsono T.;Aji M.P.;others. ;The adsorption of dye waste using black carbon from polyethylene terephthalate (PET) plastic bottle waste. *Journal of Physics: Conference Series*, 1321(2): 22011 (2019).
- [47] Doğan M.;Karaoğlu M.H.;Alkan M.;Do M.;Karao M.H.;Alkan M. ;Adsorption kinetics of maxilon yellow 4GL and maxilon red GRL dyes on kaolinite. *Journal of Hazardous Materials*, 165(1–3): 1142–1151 (2009).
- [48] Karaoğlu M.H.;Zor Ş.;Uğurlu M. ;Biosorption of Cr(III) from solutions using vineyard pruning waste. *Chemical Engineering Journal*, 159(1–3): 98–106 (2010).
- [49] Padmavathy V. ;Biosorption of nickel (II) ions by baker's yeast: Kinetic, thermodynamic and desorption studies. *Bioresource Technology*, 99(8): 3100–3109 (2008).